High-Speed, Random-Access Fluorescence Microscopy:
II. Fast Quantitative Measurements With Voltage-Sensitive Dyes

A. Bullen*[#] and P. Saggau*

*Division of Neuroscience, Baylor College of Medicine, Houston, Texas 77030, and [#]Department of Physiology, University of Pennsylvania School of Medicine, Philadelphia, Pennsylvania 19104

ABSTRACT   An improved method for making fast quantitative determinations of membrane potential with voltage-sensitive dyes is presented. This method incorporates a high-speed, random-access, laser-scanning scheme (Bullen et al., 1997. *Biophys. J.* 73:477–491) with simultaneous detection at two emission wavelengths. The basis of this ratiometric approach is the voltage-dependent shift in the emission spectrum of the voltage-sensitive dye di-8-butyl-amino-naphthyl-ethylene-pyridinium-propyl-sulfonate (di-8-ANEPPS). Optical measurements are made at two emission wavelengths, using secondary dichroic beamsplitting and dual photodetectors (<570 nm and >570 nm). Calibration of the ratiometric measurements between signals at these wavelengths was achieved using simultaneous optical and patch-clamp measurements from adjacent points. Data demonstrating the linearity, precision, and accuracy of this technique are presented. Records obtained with this method exhibited a voltage resolution of ~5 mV, without any need for temporal or spatial averaging. Ratiometric recordings of action potentials from isolated hippocampal neurons are used to illustrate the usefulness of this approach. This method is unique in that it is the first to allow quantitative determination of dynamic membrane potential changes in a manner optimized for both high spatiotemporal resolution (2 μm and <0.5 ms) and voltage discrimination.

INTRODUCTION

Existing approaches to making quantitative measurements of membrane potential using voltage-sensitive dyes (VSDs) are slow, lack spatial resolution, or exhibit poor voltage discrimination and therefore are not widely used (Bedlack et al., 1992, 1994; Gross et al., 1994; Gonzalez and Tsien, 1995, 1997; Beach et al., 1996; Zhang et al., 1998). However, the response times of typical VSDs (Loew et al., 1985; Salzberg et al., 1993) are easily sufficient to follow fast membrane events, and these probes exhibit many favorable features useful in investigating problems and/or preparations in which the use of multielectrode approaches would be difficult or impossible (for examples see Cohen and Salzberg, 1978, or Ebner and Chen, 1995). Moreover, these indicators are noninvasive and allow long-term measurements with high spatial and temporal resolution. Unfortunately, these favorable features are tempered by the fact that the signals produced from these probes typically allow only qualitative comparisons between recording sites (but see Fromherz and Muller, 1994). Commonly, the signal derived from these dyes is displayed as the change in fluorescence (ΔF) or more commonly as the change in fluorescence normalized by its mean ($\Delta F/F$). Although calculating $\Delta F/F$ is a useful way to normalize signal size, it does not allow quantitative determinations of absolute signal size (in mV) or comparisons across recording sites or between cells. More elaborate methods are required to make such quanti-

tative measurements. One possibility is ratiometric measurements (Grynkiewicz et al., 1985; Tsien and Ponnie, 1986; Dunn et al., 1994). Typically, such an approach forms a ratio of fluorescence intensities measured at different wavelengths, preferably where the signal at one wavelength is insensitive to the parameter of interest or where signals from two wavelengths vary in opposing directions. Previous studies, especially those employing fluorescent calcium indicators such as Fura-2, have shown that ratios formed in this manner exhibit many advantages over single-wavelength methods. For instance, these measurements are insensitive to localized differences in loading or staining, emission intensity, and bleaching.

This study utilizes a similar ratiometric approach to membrane potential measurement, which is based on the voltage-dependent shift in the emission spectra of the styryl dye di-8-butyl-amino-naphthyl-ethylene-pyridinium-propyl-sulfonate (di-8-ANEPPS) (Beach et al., 1996). Dyes in this class have been shown to exhibit significant voltage-dependent shifts in both excitation and emission spectra (Fluhler et al., 1985; Montana et al., 1989; Fromherz and Muller, 1993). The physical mechanism underlying this kind of shift has been termed "electrochromic" (Loew et al., 1979) and is thought to arise from charge rearrangements that mirror changes in membrane potential (Loew, 1993). The speed of this shift is likely comparable (Loew et al., 1985; Ehrenberg et al., 1987) to that of the corresponding amplitude changes also exhibited by these probes and is easily fast enough to track changes in membrane potential (Montana et al., 1989).

Previously, the excitation shifts of di-4-ANEPPS and di-8-ANEPPS have been used as the basis for static ratiometric determinations of membrane potential in various cell types and preparations (Bedlack et al., 1992, 1994; Gross et al., 1994; Zhang et al., 1998). However, these studies were

typically conducted at video rate (i.e., 30 Hz) or slower, because of the time required to process interlaced images or switch excitation filters. This shortcoming limits the usefulness of this method in investigations of membrane potential dynamics, which commonly require sampling rates greater than 1 kHz to adequately capture the signals of interest (i.e., action potentials and postsynaptic potentials). When a comparable emission ratio scheme is employed, the mechanical limitations inherent in switching excitation wavelengths can be avoided and thus higher sampling rates are possible. However, to achieve a higher temporal bandwidth, methods employing the emission shift require two independent photodetectors that can be sampled simultaneously (e.g., Beach et al., 1996); otherwise, measurements from a single detector must still be interleaved (e.g., Yuste et al., 1997) and are therefore relatively slow.

In addition to normalizing for local differences in static fluorescence and variations in local voltage sensitivity, simultaneous measurements at two emission wavelengths offer a number of other potential advantages. In particular, multiplicative noise that contaminates both wavelengths (i.e., common-mode noise) can be effectively removed in the ratio formation process. Such common-mode signals can include high-frequency intensity variations such as source noise (i.e., laser noise) or slower bleaching artifacts. Previously, the magnitude of source noise variations, relative to absolute signal sizes, has discouraged the use of laser sources in studies using voltage-sensitive dyes.

In this report, we document a significant improvement to a novel optical method that enables calibrated measurements of membrane potential to be made with high spatiotemporal resolution. Our approach utilizes the fast, high-resolution point illumination capability of a recently developed laser scanning microscope (Bullen et al., 1997) together with simultaneous detection at two wavelengths to produce high-fidelity ratiometric recordings of membrane potential. Using this methodology and patch-clamp techniques, we have quantified membrane potential changes in cultured hippocampal neurons on a subcellular level. In particular, the issues of linearity, accuracy, and precision are addressed. Furthermore, the point-to-point and trial-to-trial accuracy of this technique is verified with concurrent electrical recordings. The advantages of this approach include its large temporal bandwidth, high spatial resolution, increased voltage sensitivity, and common-mode noise cancellation. At present, this method does not correct for nonspecific fluorescence arising from adjacent stained structures. The relative contribution of this extraneous fluorescence depends on the tissue or cellular structure being studied. In particular, nonspecific fluorescence is likely to be larger in more complex preparations (i.e., brain slices or isolated ganglia) when compared to the dispersed cultures used here. However, approaches to eliminating this problem in these more complex tissues are discussed. In summary, we have shown that this method is useful for making quantitative measurements of membrane potential from distributed cellular structures in a manner not previously possible.

Preliminary reports of this work were previously published in abstract form (Bullen and Saggau, 1997a,b).

MATERIALS AND METHODS

Previously, we have described a random-access scanning system capable of high-resolution optical measurements from small neuronal structures (Bullen et al., 1997). This system was specially constructed for experimental situations requiring submillisecond temporal resolution and high spatial resolution (i.e., 2 μm). In addition, signals acquired with this instrument are digitized with 16-bit resolution, thus allowing the incorporation of optical probes with relatively poor voltage sensitivity ($<1\%$ $\Delta F/F$ per 100 mV). Here we extend this instrument to include the capability to make ratiometric determinations of membrane potential, using voltage-sensitive dyes with the same high spatiotemporal resolution and in the absence of any signal averaging.

Spectral considerations

The underlying basis of this approach to making ratiometric measurements is the voltage-dependent shift in the emission spectrum of the voltage-sensitive dye di-8-ANEPPS (Molecular Probes, Eugene, OR). The chemical structure of this probe is shown in Fig. 1 *A*. Many of the important spectral properties of this dye are described in the literature (see Haugland, 1996, for summary). However, in some cases missing values were extrapolated from di-4-ANEPPS, a structurally similar voltage-sensitive dye, which has been more fully characterized (Fromherz and Lambacher, 1991; Loew et al., 1992; Fromherz and Muller, 1993). In particular, the nature and voltage sensitivity of the emission shift for di-4-ANEPPS has been extensively documented by Fromherz and colleagues (Fromherz and Lambacher, 1991; Fromherz and Muller, 1993). Such a voltage-dependent shift results in a relative intensity change when fluorescence is sampled from discrete spectral bands. When such measurements are made from spectral bands on either side of the peak emission wavelength (i.e., 570–580 nm), these fluorescence changes occur in opposite directions. This is demonstrated schematically in a difference spectrum (Fig. 1 *B*), which was generated by subtracting an emission spectrum measured at a different membrane potential from a spectrum generated at rest. When the fluorescence intensity is monitored from spectral bands on either side of this difference spectrum and a ratio is formed between these values, the resulting measurement can be shown to be corrected for variations in signal strength and common-mode noise sources (i.e., laser noise). Furthermore, the relative change in the signal is magnified and thus the sensitivity is increased. It is important to note that this scheme represents an idealized case, and absolute spectral shifts were not determined in this study. Furthermore, other spectral changes that are dependent on membrane potential have been documented (Fromherz and Lambacher, 1991; see Limitations and Trade-Offs under the Discussion) and may cause some small deviation from this idealized scheme.

Optical methods

The microscope used in this study is essentially the same as that described by Bullen et al. (1997), with the following additions or alterations. First, additional argon laser lines (i.e., 476 nm, 488 nm, and 502 nm) were employed to closely match the peak of the absorption spectrum for this dye and to assess the relative importance of excitation wavelength in the ratio formation process. Corresponding changes in the primary dichroic mirror were made to match each of these laser lines. Second, emission light was collected using an epifluorescence configuration (Fig. 2) and further processed with a secondary dichroic mirror (DCLP570; Chroma Technology, Brattleboro, VT) and two emission filters (D540/50M and D600/60M; Chroma Technology). The optimal combination of emission filters was empirically matched to fluorescence signals arising from the preparation. Several combinations of filters and dichroic mirrors (including Q565LP,
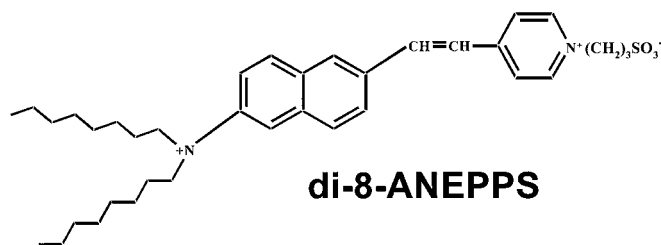
A.

di-8-ANEPPS

FIGURE 1 di-8-ANEPPS and its spectral properties. (*A*) The chemical structure of the voltage-sensitive dye di-8-butyl-amino-napthyl-ethylene-pyridinium-propyl-sulfonate (di-8-ANEPPS). (*B*) Schematic representation of spectral shifts of di-8-ANEPPS, including both excitation and emission shifts. The top panel shows measured spectrums on which published values of spectral shifts have been imposed. The difference spectra between shifted and non-shifted or resting spectra (not shown) are documented in the bottom panel. The point on the excitation difference spectrum that corresponds to the 476-nm laser line used here is highlighted with an arrow. The separate spectral bands of the emission spectrum that were sampled in this study are shown by the cross-hatched regions.

B.

Excitation Spectra

Emission Spectra

Spectral shifts due to voltage transients

Difference spectra
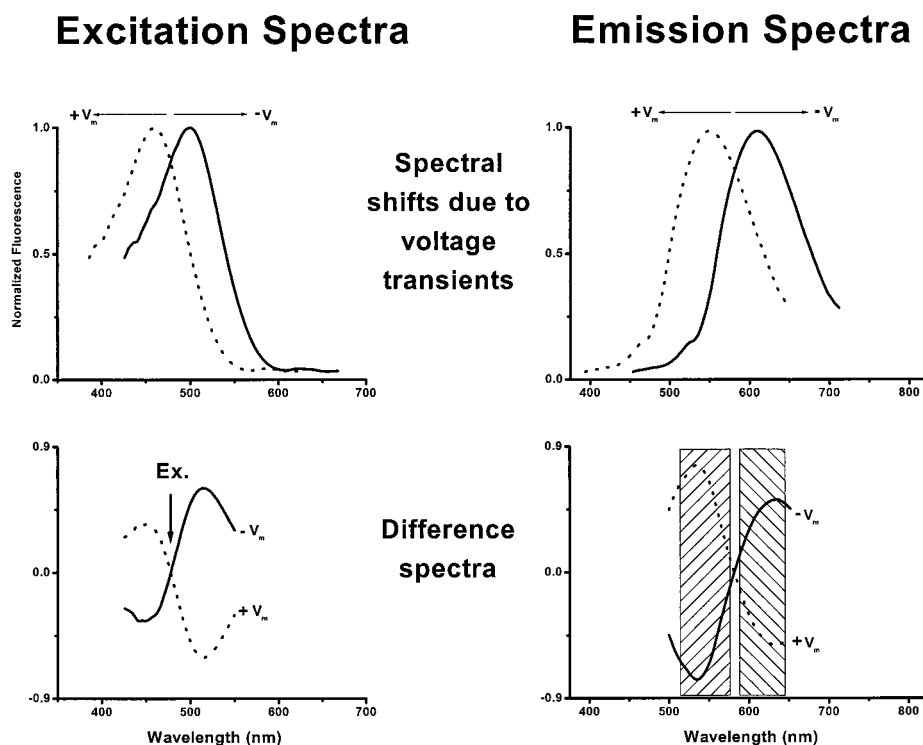
DCLP570, DCLP580, DCLP595, D550/50M, HQ535(50)X, HQ545(80), 535DF45, D585/30M, OG590, OG570) were tested before the final selection was chosen based on signal strength and spectral considerations. Corresponding differences in signal handling for this optical scheme are described below.

In all cases, spatial resolution, as dictated by scanning spot size at the level of the preparation, was equal to 2 μm. Typically, the optical signals presented here were sampled at 3 kHz, digitized with 16-bit resolution, and digitally filtered at 1.0 kHz or less, depending on the interesting signal characteristics.

Signal processing

Multistage signal processing is required for ratio formation and noise reduction. A scheme describing various levels of signal manipulation is depicted in Fig. 2. In brief, two fluorescent signals are captured by a pair of equivalent photodetectors. Each of these detectors is simultaneously sampled during the time the laser beam "dwells" at a particular recording site. These measurements are then digitized and a ratio is formed between

these corresponding observations. A complete time-dependent record for each individual recording site is then reconstructed, on a point-by-point basis, from the ratio measurements that had been made at all recording sites and interlaced together.

In other cases, signals were processed as in Bullen et al. (1997) to illustrate the relative efficacy of different signal processing methods. This signal processing method involved sampling the relative intensity fluctuations directly from the laser source with a reference photodetector. Later, a ratio is formed between excitation and emission signals to remove variations in laser intensity (see Bullen et al., 1997, for details). However, in the present case, in which two fluorescent signals are monitored, each one contains these fluctuations and they are conveniently removed during the ratio formation process. Hence an additional reference detector is no longer required in emission ratio formation.

Regardless of which signals were used for ratio formation, additional uncorrelated or random noise arising from each photodetector was removed in a final digital filtering step.

Calibration of this ratio was achieved using simultaneous optical and patch-clamp measurements from adjacent points. For calibration experi-

FIGURE 2 Optical and signal processing scheme. This is a schematic representation of the optical and signal processing steps used in this study to produce ratiometric recordings. Individual fluorescence measurements are made simultaneously at two emission wavelengths during the time the laser beam "dwells" at each individual recording site. Fluorescence records ($\Delta F/F$) for each spectral band ($\Delta F/F_{<570}$ and $\Delta F/F_{>570}$) are shown in the left and right boxes, respectively. These records are dotted to depict the point-by-point sampling. Complete time-dependent records for each recording site are later demultiplexed from serial records of all such points (and emission wavelengths). Ratio formation and filtering are completed digitally before the records are displayed interactively as R/R. Normalization and calibration are typically accomplished off-line after determination of $R_{abs(0)}$. The final normalized and calibrated trace is shown in the bottom box. Laser lines used included 476 nm, 488 nm, and 502 nm. Primary dichroic mirrors used included DCLP485, DCLP495, and DCLP525. The secondary dichroic mirror used was DCLP570. Emission filters used were 540/50 nm (EM_1) and 600/60 nm (EM_2).
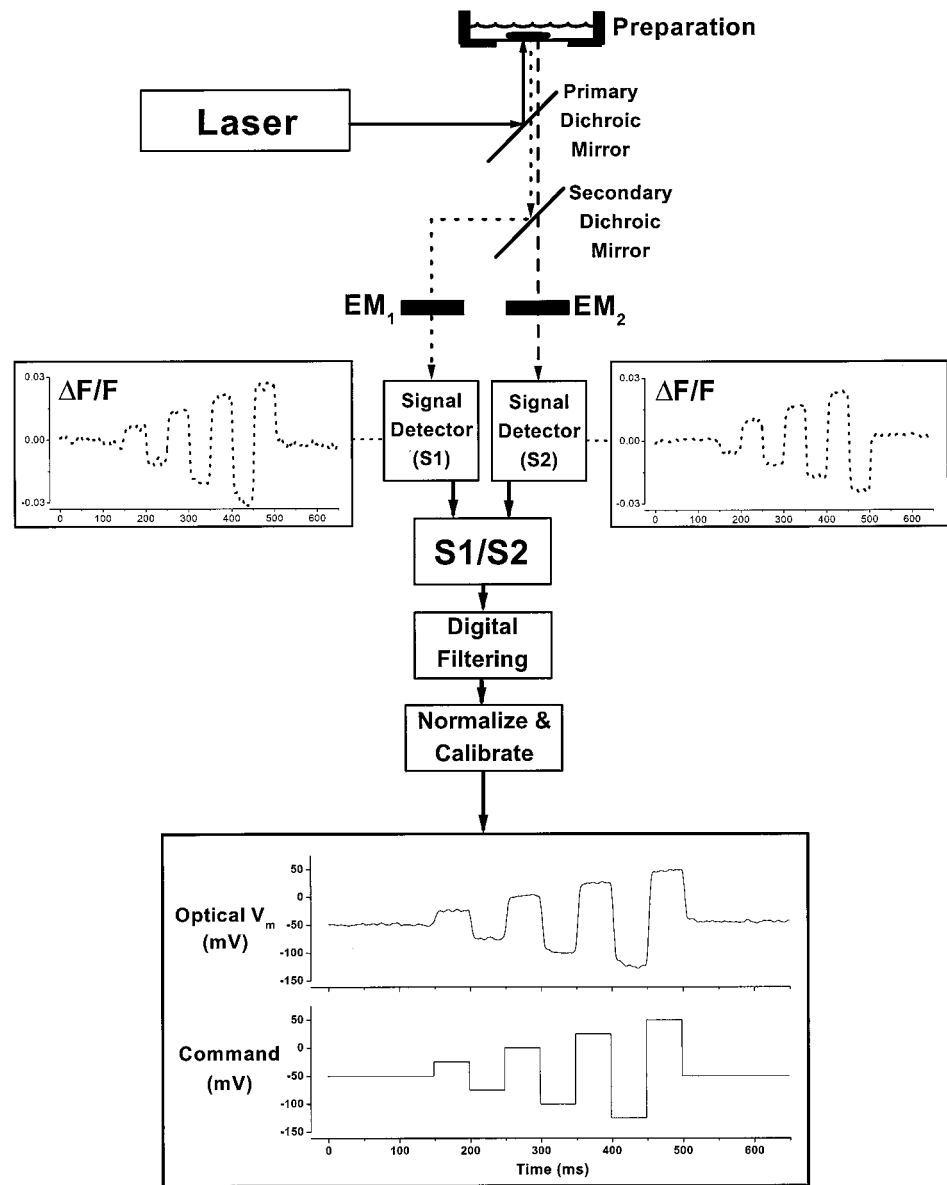
ments, 8–12 trials were averaged together to minimize any errors caused by trial-to-trial variability or random noise.

Patch clamp

An Axon Instruments (Foster City, CA) Axopatch 200A amplifier was used for both voltage- and current-clamp experiments described below.

Voltage clamp

The calibration of optical signals was achieved with a series of voltage steps generated via a somatic patch pipette under voltage-clamp control. These determinations were made under conditions that favor good space clamp and accurate voltage control. In particular, all active conductances were blocked pharmacologically, and large pipettes with small series resistances ($R_{electrode}$ = 2–3 MΩ) were employed. Whole-cell currents were also monitored to ensure good clamp performance. Optical measurements were always made between 5 and 10 μm from the patch pipette. For experiments examining spatial differences in the optical signals, patch

recordings were made directly on dendritic branches ($R_{electrode}$ = 3–4 MΩ).

Current clamp

Membrane potential signals were acquired via whole-cell patch recordings ($R_{electrode}$ = 2–4 MΩ) undertaken in current-clamp mode using the "I-Clamp normal" mode of the Axopatch 200A amplifier. Electrical signals were prefiltered at 2 kHz and digitized at 7.5 kHz (12-bit digitizing resolution). Perforated patch recordings were made to minimize any change in intracellular ion concentrations and avoid washout of any intracellular constituents. Briefly, a Nystatin or Amphotericin (both Sigma) stock was made fresh each day (15 mg/ml in a 20:1 solution of dimethyl sulfoxide/Pluronic-F127). For each experiment, 10 μl of this stock was added to 1 ml of pipette solution (see below) for a final concentration of 150 μg/ml. This solution was typically used for 2–3 h after which fresh solutions were made. Filtered antibiotic-containing solution was used to backfill a regular patch pipette that had previously been tip-filled with bath saline. Action potentials were evoked by current injection (50–100 pA)

Solutions

Bath saline for all experiments was (in mM) 140 NaCl, 2 CaCl$_2$, 4 KCl, 1 MgCl$_2$, 10 HEPES, 10 D-glucose (pH 7.3). The pipette solution for voltage-clamp experiments was (in mM) 120 CsCl (or CsF), 10 TEA-Cl, 5 4-AP, 2 QX-314, 10 EGTA, 10 HEPES (pH 7.4). In addition, the following drugs were added to the bath solution during voltage-clamp experiments (in μM): 1 tetrodotoxin, 2000 TEA, 1000 4-AP, 10 CNQX, 25 APV, and 50 Cd. The pipette solution for current-clamp (perforated patch configuration) experiments was (in mM) 110 K sulfate, 5 NaCl, 20 KCl, 10 EGTA, 10 HEPES (pH 7.4 w/− KOH).

Cell preparation and staining

Hippocampal neurons were harvested from E19 rat pups and dissociated using a modified version of the protocol outlined by Brewer et al. (1993). These cells were plated on an optically clear fluoropolymer film (ACLAR 33C; Allied Signal, Pottsville, PA) at a density of 50–60 cells/mm^2. These cells were maintained in serum-free medium (B27/NEUROBASAL mix; Life Technologies, Grand Island, NY) in a water-saturated atmosphere of 95% air and 5% CO$_2$. Cells were used between 1 to 4 weeks in culture. Previous studies (Goslin and Banker, 1991) have documented how cells cultured at this stage are mostly pyramidal neurons with a well-characterized pattern of development. After 3 days in culture these cells become polarized, with one small axon and many larger, tapering dendrites.

Stock solutions of di-8-ANEPPS were made up in a DMSO/Pluronic-F127 (3:1) solution and stored at 4°C (Rohr and Salzberg, 1994a,b). Cells were stained (5–15 min) by bath application of 20–100 μM di-8-ANEPPS in bath saline. Excess dye was removed by several washes in bath saline. In some cases, an antioxidant combination of glucose oxidase (40 units/ml; Sigma, St Louis, MO), catalase (800 units/ml; Sigma), and Trolox C (100 μM; Aldrich, Milwaukee, WI) was used to prevent photodynamic damage generated by reactive oxygen species (see Obaid and Salzberg, 1997, and Scheenen et al., 1996).

RESULTS

Simultaneous voltage-clamp and optical recordings were made from hippocampal neurons to assess the nature, linearity, accuracy, precision, and variability of ratiometric fluorescence determinations based on measurements made from two spectral bands. In addition, the spatial homogeneity of fluorescence signals arising from different cellular structures was investigated. Finally, the suitability of this method for making spatially resolved membrane potential recordings, in the absence of voltage-clamp control, was assessed.

Normalized fluorescence signals

Fluorescence signals measured from each spectral band varied systematically in a manner consistent with the difference spectrum depicted earlier (Fig. 1 *B*) and described in previous studies (Fluhler et al., 1985; Beach et al., 1996; Yuste et al., 1997). Specifically, a transient depolarization was accompanied by a decrease in fluorescence intensity above 570 nm ($F_{>570}$). A corresponding increase was observed in the signal measured below 570 nm ($F_{<570}$). As can be seen from Fig. 3 *A*, the relative magnitude of $\Delta F/F$ at each wavelength is similar ($\lambda_{\text{Excit}} = 476$ nm), demonstrating a comparable level of voltage sensitivity. Formation of the ratio between these measurements ($F_{<570}$ and $F_{<570}$)

produces an absolute ratio (termed R_{abs}) that is linearly related to the membrane potential (Fig. 3 *B*). By virtue of the fact that individual emission measurements change in opposite directions, the relative magnitude of the R_{abs} (depicted as $\Delta R_{\text{abs}}/R_{\text{abs}}$) and hence its voltage sensitivity were greater than at either wavelength alone. An additional feature of this ratiometric approach, also demonstrated in Fig. 3 *A*, is the correction of bleaching that occurs equally in each record. Similarly, other common-mode or multiplicative noise sources such as laser noise are conveniently canceled out during this procedure (not shown).

An important goal of this study was to generate a conversion factor for this particular dye to transform R_{abs} into an absolute change in membrane potential (in mV). When a large number of similar recordings (Fig. 3 *B*) were made from equivalent cells, it became apparent that, although the relationship (i.e., slope) between R_{abs} and membrane potential remained approximately constant, there was considerable cell-to-cell variability in its absolute magnitude (or offset). For this reason, a normalized parameter (R_{norm}) was derived whereby each value of R_{abs} was corrected by subtraction of R_{abs} at zero mV ($R_{\text{abs}(0)}$). Fig. 4 *A* demonstrates this procedure for a single experimental record. An array of similar traces is presented in Fig. 4 *B*. This panel documents the variability in the offset of R_{abs} from many recordings taken from many similar cells under identical recording conditions.

Several other important features of the ratio formation process are apparent from this figure. First, although each record indicates that $\Delta F/F$ is linearly related to membrane potential, this relationship is obviously different in slope across recording sites and cells. This is one reason why it would be inappropriate to use this parameter to make quantitative comparisons between points and across cells. Second, the variability in voltage sensitivity (or slope) of $\Delta F/F$ is corrected by the ratio formation process, as all R_{abs} records possess approximately the same slope. Unfortunately, variations in the local fluorescence intensity due to staining differences or the underlying cellular structure (and possibly differences in illumination efficiency) mean that R_{abs} can be offset by varying amounts. Under these conditions any global calibration factor used to convert R_{abs} for a single sweep record would be quite inaccurate. However, correcting R_{abs} by $R_{\text{abs}(0)}$ effectively removes this offset and produces a family of lines with similar slope and offset (Fig. 4 *B*, *bottom panel*). When group means are derived from many similar experiments the relative variability in R_{norm} is quite small (and less than $\Delta F/F$; Fig. 4 *C*, *bottom panel*), and hence under experimental conditions this relationship can conceivably be used, with an appropriate conversion factor, to infer absolute changes in membrane potential with less chance of error. Group data from many similar cells (Fig. 4 *C*) indicate that under the conditions used here this conversion factor would be 100 mV/0.015 with 0 mV membrane potential set at $R_{\text{norm}} = 0$.
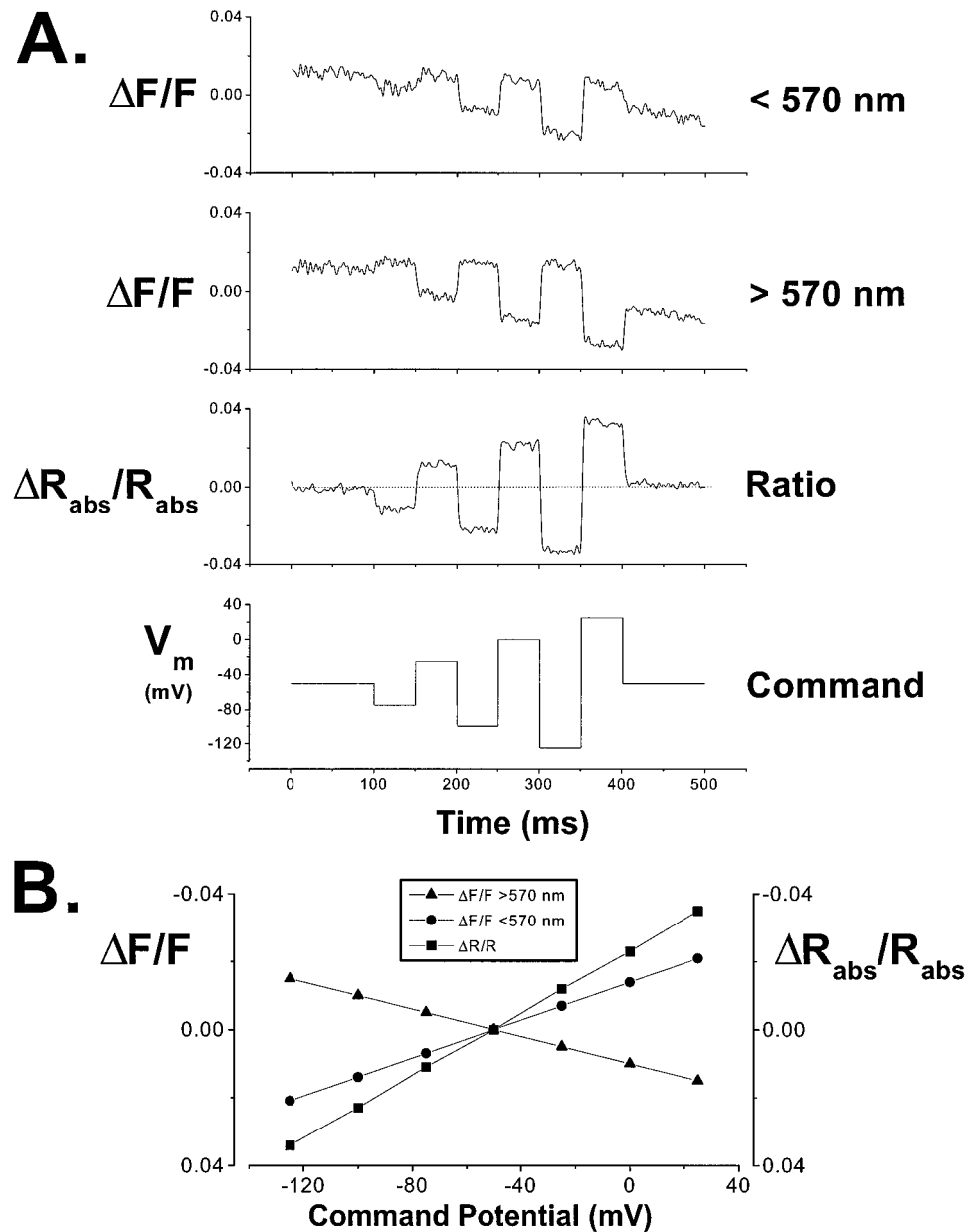
FIGURE 3 Ratiometric membrane potential signals. Optical signals were recorded under voltage-clamp conditions from single recording sites in cultured hippocampal neurons. (*A*) Comparison of $\Delta F/F$ at different emission wavelengths and the corresponding ratiometric measure (R_{abs}) generated from dividing $F_{<570}$ by $F_{>570}$. Records ($n = 1$) with an unusually high level of bleaching were selected to illustrate the efficacy of bleaching correction with this method. $\Delta F/F$ records were corrected for laser noise, using a reference signal, as in Bullen et al. (1997). (*B*) A comparison of $\Delta F/F$ at each wavelength and the relative change in the ratio (i.e., $\Delta R_{abs}/R_{abs}$) plotted on the same scale. Note the larger dynamic range apparent in the ratio when compared to either single-wavelength measurement.

Effect of holding potential

Another limitation arising from the use of the parameter $\Delta F/F$ is that it is somewhat dependent on the resting level and waveform shape. Specifically, the absolute value of $\Delta F/F$ and/or baseline has no physiological significance and is determined in large part by the waveform shape measured. In experiments designed to show the efficacy of R_{norm} in overcoming this problem, a series of similar membrane potential manipulations were undertaken from different holding potentials (see Fig. 5 *A*, *Command*). In each case, the size and offset measured by the R_{norm} parameter successfully reproduced the command waveform (Fig. 5 *B*, *bottom panel*). In contrast, whereas the slope of $\Delta F/F$ was conserved, its baseline was shifted, depending on holding potential and waveform shape. Although an equivalent cal-

ibration of $\Delta F/F$ is theoretically possible, both the slope and offset of the $\Delta F/F$ versus V_m relationship would have to be determined for each individual recording site.

Precision of ratiometric measurements

Absolute voltage resolution is an important consideration in assessing the viability of this approach. To determine the precision or resolution possible with this method, experiments were undertaken to determine the smallest resolvable step that could be reliably measured with ratiometric recordings ($\Delta R_{abs}/R_{abs}$). Fig. 6 documents representative records from experiments of this type. In each case the criterion for distinguishing the minimum step size was whether each step could clearly be separated from a baseline
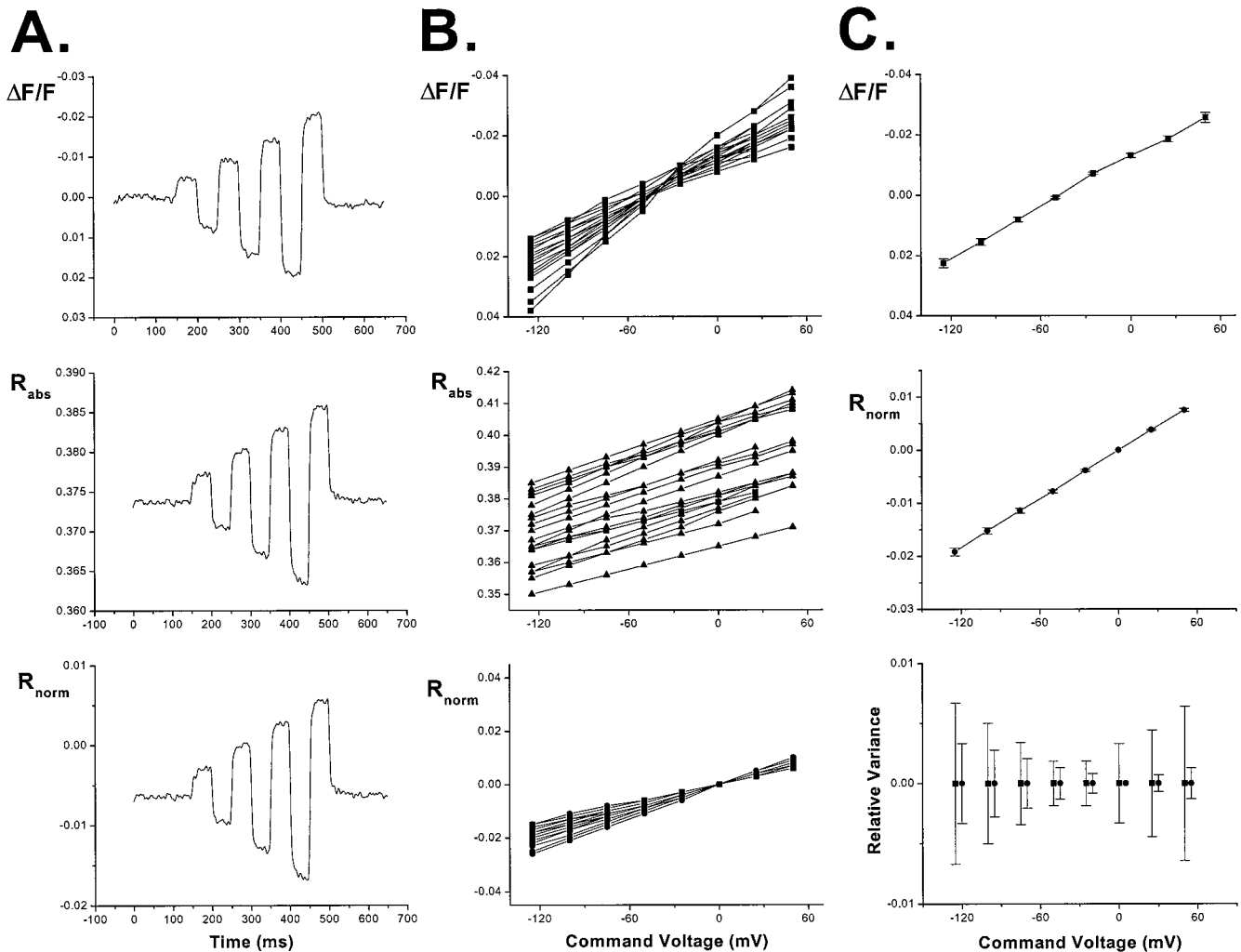
FIGURE 4   Normalized ratiometric membrane potential signals. (*A*) Representative records of $\Delta F/F$, R_{abs}, and R_{norm} taken from the same recording point. Voltage steps (multiples of 25 mV) were elicited from a holding potential of -50 mV. Excitation wavelength $= 488$ nm. (*B*) Representative records of $\Delta F/F$, R_{abs}, and R_{norm} taken from many similar cells demonstrating the variability slope (and therefore voltage sensitivity) of $\Delta F/F$. The variability in slope is overcome by the formation R_{abs}; however, there is considerable variability in the offset of R_{abs}. Normalization of R_{abs} by subtraction of $R_{abs(0)}$ to give R_{norm} demonstrates a common slope and offset relative to membrane voltage. (*C*) Group data (mean $\pm$ SEM; $n = 18$) demonstrating the linear relationship and low variability between R_{norm} and membrane potential. A comparison of relative variance between $\Delta F/F$ ■ and R_{norm} ● is documented in the bottom panel.

measurement measured from the same point under the same recording conditions. On average the smallest resolvable step measured was between 2.5 and 5 mV in averaged data ($N \leq 8$) and ~5 mV for single sweep records. This value closely corresponds to variability documented in the group data presented earlier. Hence both the variability inherent in making these measurements and the best possible precision achievable indicate a voltage resolution of ~5 mV in single trials.

Effect of altering excitation wavelength

One advantage of the laser-scanning approach used here was the capability of employing a discrete laser line for excitation purposes. Initially we positioned this line to coincide with the peak of the on-membrane absorption spectra

of di-8-ANEPPS (i.e., 476 nm). This point is also the least sensitive to changes in fluorescence arising from the voltage-dependent shift in the excitation spectrum, as indicated in Fig. 1 (i.e., excitation difference spectra). However, because this line is relatively weak and even unavailable in some lasers, we chose to examine the effect of changes in excitation wavelength on R_{norm}. Over a range of excitation wavelengths (i.e., 476 nm, 488 nm, and 502 nm), R_{norm} exhibited a relatively constant sensitivity to membrane voltage. As shown in Fig. 7*B* (*bottom panel*), there were no significant differences in this relationship between excitation wavelengths 476 and 488 nm. Excitation with a 502-nm laser line revealed a small difference in voltage sensitivity when compared to the other lines, but this effect was barely significant when the variability between cells was taken into account. However, an interesting relationship was noted
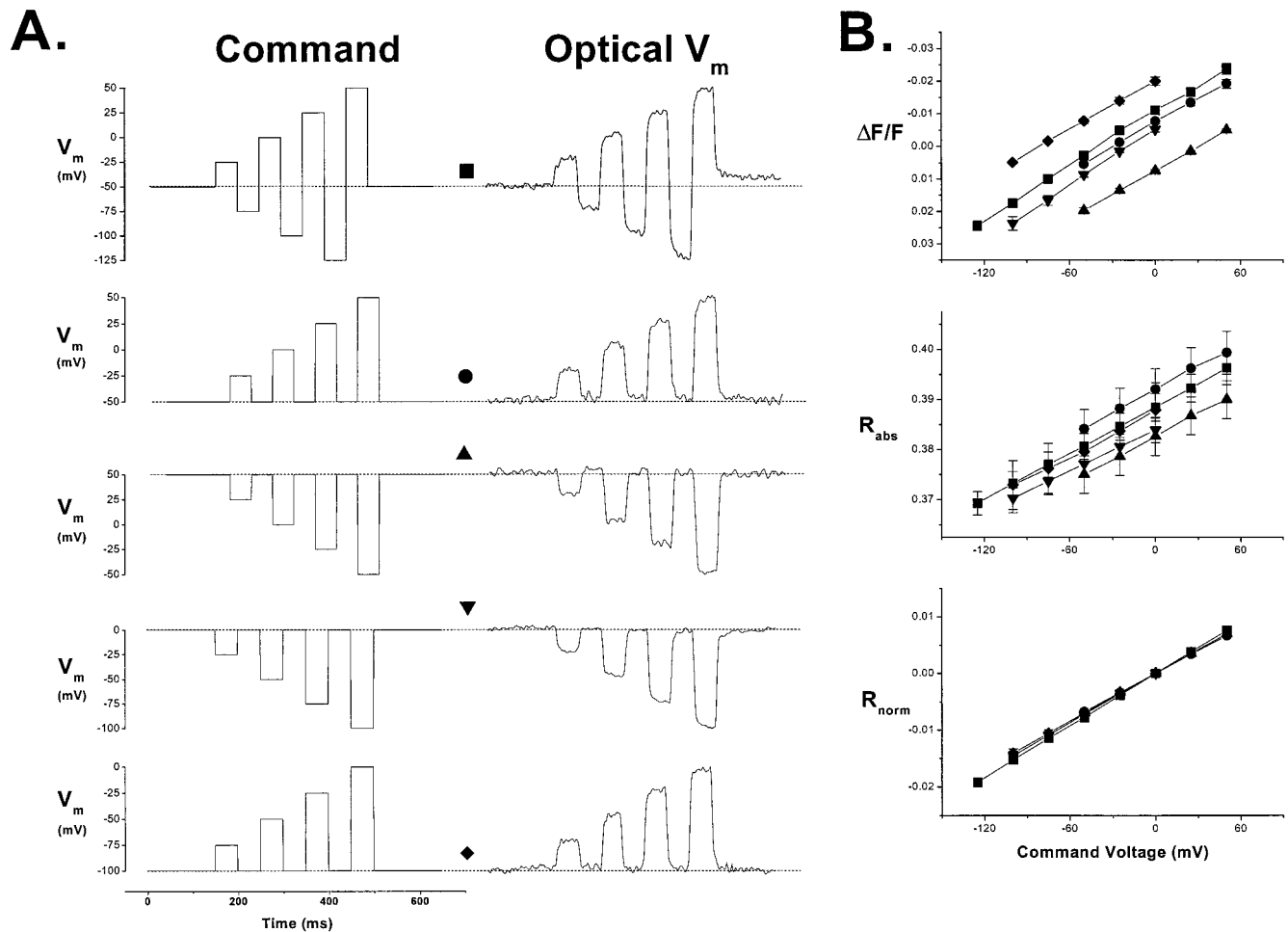
FIGURE 5   The effect of waveform shape and holding potential on $\Delta F/F$ and R_{norm}. (*A*) Individual records (R_{norm}) of experiments employing various voltage-clamp protocols (Command). Voltage steps (multiples of 25 mV) were elicited from a range of holding potentials (given at the *left*). Data are from different cells in each case. (*B*) Group data from many similar experiments. Note that whereas the slope of $\Delta F/F$ with respect to the command potential is similar, the offset and zero point vary, depending on the holding potential and waveform shape. In contrast, R_{norm} is independent of the holding potential and waveform shape. $n = 20$ (■), 10 (●), 11 (▲), 16 (▼), and 9 (♦).

between the relative voltage sensitivity of $\Delta F/F$ and excitation wavelength (Fig. 7 *B, top panel*). As the excitation wavelength was shifted further away from the peak of the excitation spectrum, the relative change in fluorescence intensity above 570 nm became larger, whereas the corresponding signal below this point became smaller, indicating decreased voltage sensitivity at that wavelength. This contrasts with measurements made at the peak of the excitation spectrum (i.e., 476 nm), where each emission wavelength exhibited roughly equal voltage sensitivity but opposite polarity. This observation likely arises from the spectral shift in the excitation spectrum that becomes more pronounced as the excitation wavelength is moved away from the peak of the absorption spectrum and begins to contribute an increasing fraction of the observed fluorescence change. Although our observations indicate that R_{norm} is relatively intolerant to small changes in excitation wavelength, it also suggests that the greatest voltage sensitivity of the ratio likely arises at the peak of the excitation spectrum. A further

practical implication of this result is that at 476 nm a better signal-to-noise ratio is obtained in both signals contributing to the ratio, and therefore under these conditions cleaner experimental records of R_{norm} are more likely. This contrasts with the single-wavelength case, in which the largest and cleanest signals arose from longer wavelength excitation (e.g., 514 nm; data not shown).

Accuracy of ratiometric recordings

Tests of the accuracy and trial-to-trial variability of our ratiometric measurements were conducted to determine whether comparisons across trials, recording sites, and cells were feasible. In each case, the variability in $\Delta F/F$, R_{abs}, and R_{norm} was examined, and the dependent variable used to compare these parameters was their voltage sensitivity or the slope of the line (parameter versus command potential), as determined by a best linear fit. In some cases, the offset

A. Single Sweep

FIGURE 6   Resolution of ratiometric recordings. (*A*) Measurements of the minimum resolvable step size as compared to baseline recorded in a single sweep measurement ($\Delta R_{abs}/R_{abs}$) under voltage-clamp conditions. Command step sizes are shown below each set of records. Each transient record is compared to a baseline measured from the same recording site under identical recording conditions. Each trace was recorded from a single 2-μm recording site. (*B*) Measurements of the underlying minimum resolvable step size from averaged records. Both voltage-clamp steps and baseline records were an average of eight records from the same recording site. Records are from different cells than in *A*, but they were made under similar conditions.
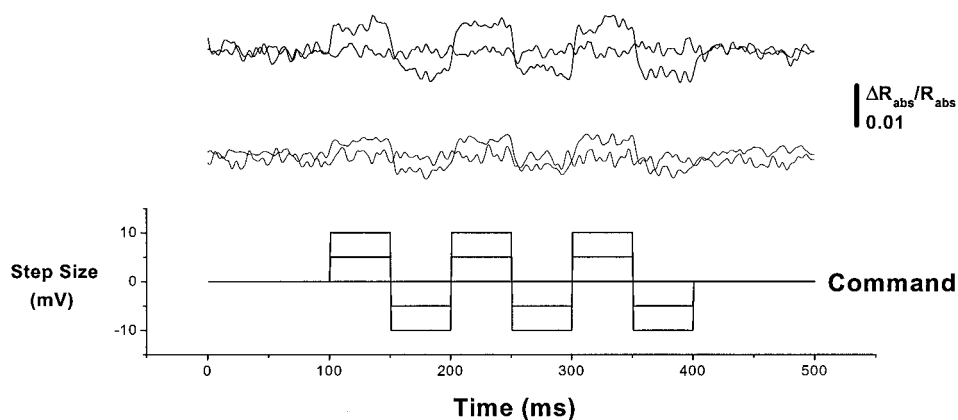
B. Averaged (n=8)
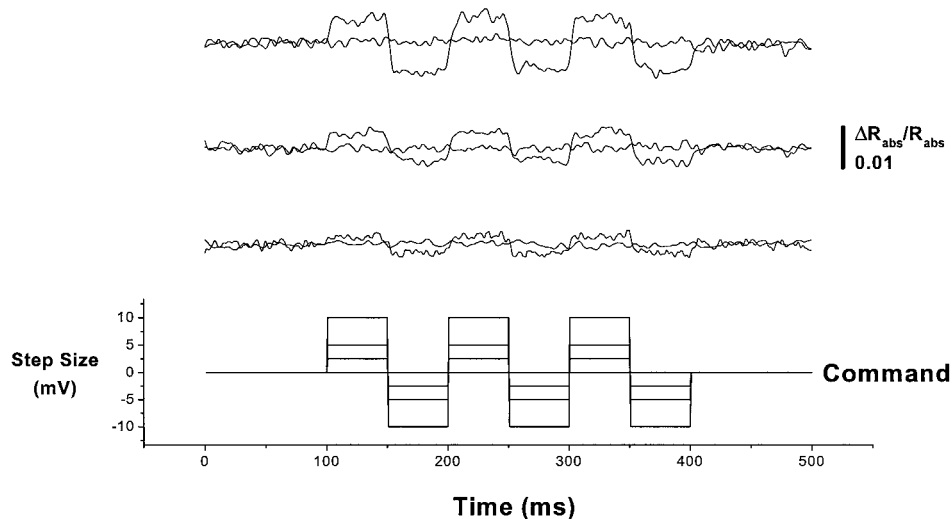
of these lines was also compared ($\Delta F/F_{(0)}$, $R_{abs(0)}$, or $R_{norm(0)}$). For these tests, it was assumed that each recording site was functionally equivalent (i.e., was equally well voltage clamped and experienced the same membrane potential). Statistical tests ($p < 0.05$) of trial-to-trial variability in voltage sensitivity conducted on a subset of data from Fig. 7 ($\lambda_{Excit} = 476$ nm) indicated that there were no significant differences for $\Delta F/F$, R_{abs}, or R_{norm}. However, one-way analysis of variance of the voltage sensitivity (or slope) between points revealed significant differences for $\Delta F/F$ but not R_{abs}. In contrast, the differences noted in the offset of R_{abs} across recording sites were significant. After correction with $R_{abs(0)}$, a similar analysis of R_{norm} revealed no significant differences in voltage sensitivity or offset from functionally equivalent sites. Because each recording site is normalized with $R_{abs(0)}$ and this parameter exhibits considerable variability, it is necessary for calibration purposes to

determine this value independently for each site, which can easily be achieved by chemically collapsing the membrane potential to zero with pore-forming ionophores (see Practical Aspects of Ratiometric Calibration under the Discussion). After independent calibration of each site, the accuracy of this technique is essentially limited to the precision of R_{norm} (see Precision of Ratiometric Measurements under the Results) and inherent variability exhibited in the group data, which were similar and quite small (~ 5 mV). In summary, observations made from equivalent points (i.e., somatic sites adjacent to patch pipette) in the same cell indicate that each recording site needs to be calibrated separately (i.e., through measurement of $R_{abs(0)}$) and calibration from one point on a cell cannot be applied to other points in the same cell. However, when signals are adjusted to determine R_{norm}, the accuracy of these measurements can be quite high.
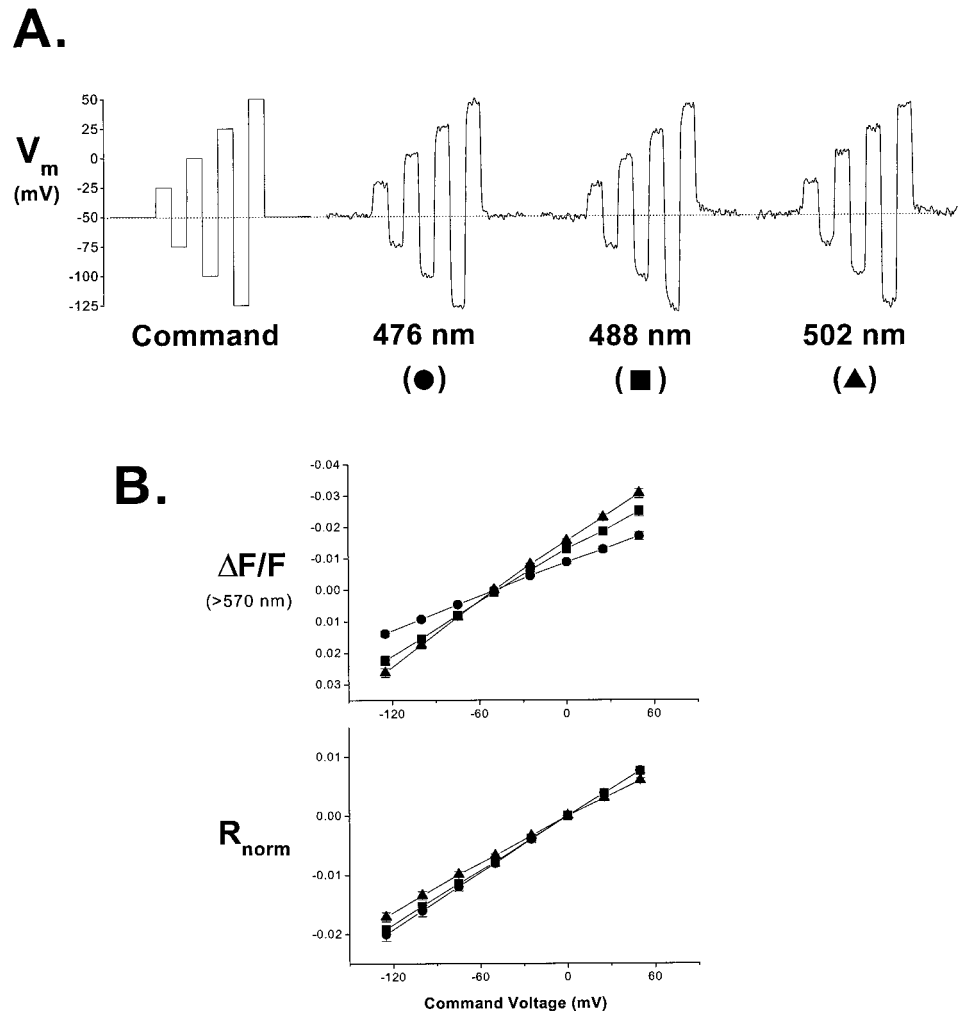
A.

FIGURE 7 Effect of excitation wavelength of R_{norm}. (*A*) Representative records of R_{norm} from experiments examining the effect of excitation wavelength on R_{norm}. Voltage steps (multiples of 25 mV) elicited from a holding potential of -50 mV are shown on the left (Command). (*B*) Group data (mean $\pm$ SEM) from many similar experiments examining $\Delta F/F$ and R_{norm}. Note how the voltage sensitivity of $\Delta F/F$ is influenced by excitation wavelength, whereas R_{norm} is relatively unaffected. $n = 17$, 20, and 15 for the wavelengths 476 nm, 488 nm, and 502 nm respectively.

B.

Regional differences in calibration

The previous section exclusively examined somatic recording sites immediately adjacent to the patch pipette. To be universally applied throughout the whole cell, any conversion factor must be consistent across different cellular structures. To test this requirement we applied voltage-clamp manipulations to various cellular structures that were amenable to seal formation with a patch pipette. Three types of structures were chosen: soma, proximal dendrite (within 20 μm of the soma), and distal dendrite (farther than 30 μm from the soma). The results of these experiments are documented in Fig. 8. In short, we found no significant differences in the voltage sensitivity of R_{norm} between these different points. It was therefore concluded that a single conversion factor (or slope) could be applied throughout the whole cell after a site-specific $R_{abs(0)}$ had been determined.

Current-clamp records

The suitability of this method for making spatially resolved membrane potential recordings, in the absence of voltage-clamp control, is demonstrated in Fig. 9. This figure indi-

cates that, under current-clamp conditions, a ratiometric signal (Fig. 9 *A*) can be recorded and calibrated to give a measurement that is highly correlated in size and offset (Fig. 9 *B*) with concurrent electrical recordings. The accuracy of this record is demonstrated by the fact the calibrated optical record varies from the electrical record in absolute magnitude by no more than the precision (5 mV) measured earlier. In summary, this figure (and data from Fig. 8) demonstrates how single-sweep (i.e., no averaging) signals of this type can be measured in a spatially resolved manner and transformed (with appropriate calibration procedures) to give quantitative information about membrane potential events in different parts of the cell.

DISCUSSION

In this report, we present an extension of a high-speed, random-access, laser-scanning system (Bullen et al., 1997) configured to make ratiometric measurements of membrane potential, utilizing the voltage-dependent emission shift of the voltage-sensitive dye di-8-ANEPPS. This instrument was specifically designed to record quantitative voltage
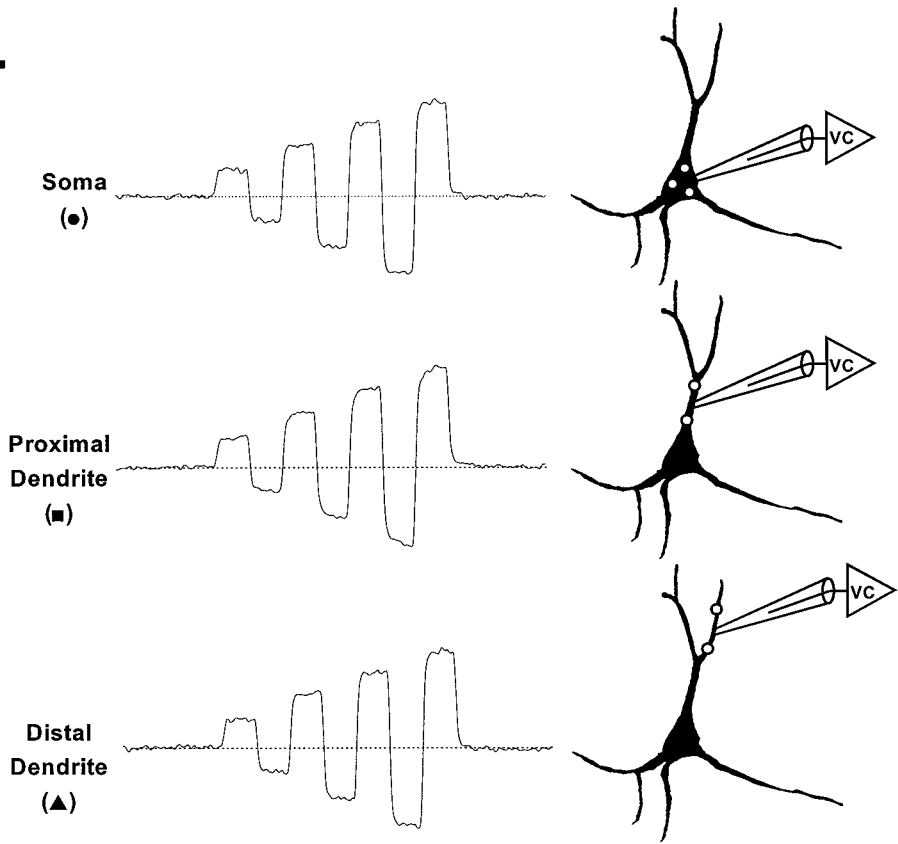
FIGURE 8 Regional differences in R_{norm}. (*A*) Representative records of signals (R_{norm}) collected under voltage-clamp conditions from spatially separated recording sites in hippocampal neurons. The relative position of each recording type is shown schematically by the graphic at the right. Voltage steps (multiples of 25 mV) were elicited from a holding potential of -50 mV and plotted on the same scale. Excitation wavelength $=$ 476 nm. (*B*) Group data (mean $\pm$ SEM) comparing the responsiveness of R_{norm} to membrane potential manipulations at different sites within isolated hippocampal neurons. Note there appears to be no significant regional differences. $n = 17$ (soma), 9 (proximal dendrite), and 7 (distal dendrite).
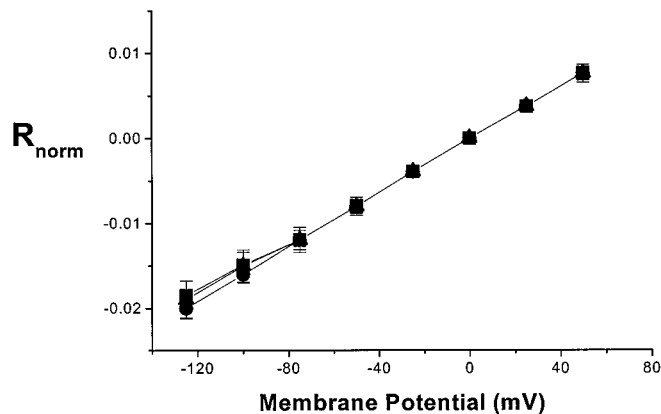
signals from small neuronal structures and has three main features that distinguish it from equivalent methods currently in use. These include a high temporal resolution (<0.5 ms), a high spatial resolution (2 μm), and a superior level of voltage discrimination (~ 5 mV). In addition, this microscope is unique because it incorporates laser illumination in a manner compatible with long-term VSD recordings (i.e., high peak illumination intensity but low average intensity). Moreover, by employing a discrete laser line whose wavelength is at or close to the voltage-insensitive point of the excitation-difference spectra (see Fig. 1), we have minimized the contribution of the voltage-dependent shift in the absorbance spectrum as a confounding influence

in our calibrations. Hence the calibrations derived with this approach will likely be more accurate than comparable methods based on the excitation shift and using broadband detection. Furthermore, we have systematically verified the accuracy, precision, and holding potential independence of this type of membrane potential measurement.

This method represents a significant advance, especially in terms of temporal bandwidth, over equivalent optical methods employed to make calibrated measurements. Moreover, this method allows the generation of spatially resolved membrane potential signals whose quality is comparable to that of electrical measurements recorded with traditional microelectrode approaches. Although currently

A.

FIGURE 9 Representative ratiometric measurements recorded from cultured hippocampal neurons using di-8-ANEPPS under current-clamp conditions. (*A*) Comparison of optical (normalized and calibrated) and electrical records measured simultaneously from adjacent recording sites (perforated patch configuration). Note: The differences between optical and electrical records is within the 5-mV voltage precision documented earlier under voltage-clamp conditions. (*B*) Correlation of optical and electrical records plotted in *A*.

B.
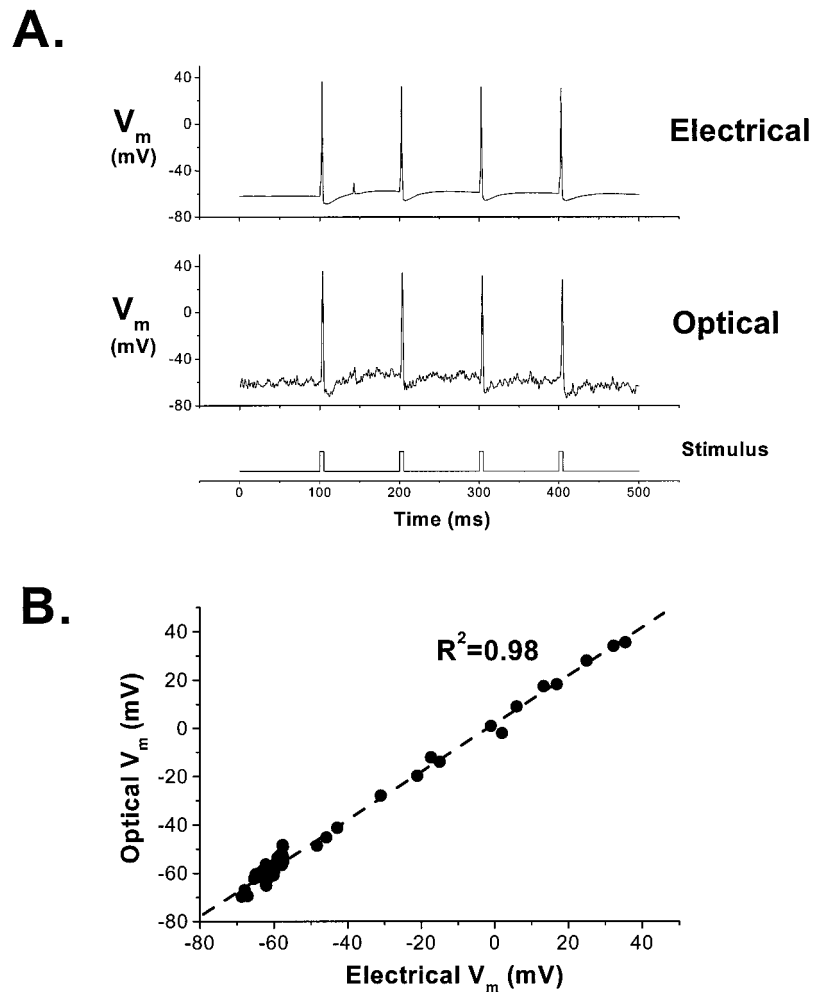
the voltage discrimination of this optical measurement technique is somewhat less than comparable electrical recording methods, it should be noted that with foreseeable advances in dye and detector technologies, a significant improvement in optical signal quality seems likely. Moreover, it is important to note that this optical method is considerably less invasive than conventional micropipette techniques.

Advantages of ratiometric measurements

When compared to typical methods for processing optical signals such as formation of ratio $\Delta F/F$, the parameter R_{norm} has several advantages in its favor. These advantages are summarized in Table 1 and can be classified into three main types: signal normalization, common-mode noise cancellation, and voltage calibration. Like normalization via $\Delta F/F$, this ratiometric method adjusts for variability in static fluorescence that can arise from staining differences and variations in cell structure. In addition, this emission ratio method also compensates for differences in the local sensitivity of VSDs to membrane potential because it is more sensitive to membrane potential and less sensitive to other confounding variables. This property arises because the

voltage-dependent component(s) of the optical signals that form this ratio vary proportionally and in opposite directions. Thus, when a ratio is formed from these fluorescence signals, voltage-independent components, which typically vary in the same direction, are conveniently canceled out. Concurrently, the voltage-sensitive component(s) of the ratio is amplified by this procedure, endowing it with relatively greater voltage sensitivity. The efficacy of this ratiometric technique in isolating voltage-sensitive signal

TABLE 1 Advantages of ratiometric emission measurements over $\Delta F/F$

	$\Delta F/F$	Ratiometric emission measurements
Normalizes for differences in static fluorescence	Yes	Yes
Normalizes for differences in local sensitivity	No	Yes
Laser and common-mode noise cancellation	No	Yes
Bleaching correction	No	Yes
Voltage sensitivity	Standard	Increased
Calibration	No	Yes

components and excluding common-mode signals is apparent from a range of experiments examining trial-to-trial variability (Fig. 4) and the effect of different stimulus parameters (waveform shape and holding potential), as documented in Fig. 5. In each case, the ratiometric parameter R_{norm} was able to accurately reproduce both resting and transient membrane potential levels. This capability allows experimental comparisons to be reliably made between recording sites, even those demonstrating large differences in electrical behavior.

In contrast, the relationship between the baseline or offset in $\Delta F/F$ and membrane potential was shown to depend, in part, on holding (or resting) potential and waveform shape. Because $\Delta F/F$ is sensitive to these differences in holding potential and waveform shape, quantitative comparisons across experimental manipulations or stimulus conditions are obviously inappropriate. Thus $\Delta F/F$ cannot to be used to determine absolute resting or transient voltage levels and instead should only be used to infer relative changes in membrane potential.

Common-mode noise cancellation is a particularly important feature of our ratiometric method. Extraneous signal components that are common to each spectral band effectively cancel out, thus producing a higher signal-to-noise ratio than otherwise possible. Such extraneous components can include source noise, movement artifacts, and bleaching artifacts. These types of artifacts are commonly seen in biological experiments in which signals are weak and susceptible to such contamination or in preparations expressing contractile behavior. Noise cancellation is particularly important in cases in which signal sizes are small and relatively noisy excitation sources, such as lasers, are employed. In addition, this common-mode cancellation feature significantly simplifies the instrumentation requirements (i.e., extremely stable light sources) of these indicators. These signal normalization and noise reduction features, together with the increased voltage sensitivity of this ratio, make it possible to make calibrations directly from these optical signals.

Practical aspects of ratiometric calibration

The finding that different recording sites within the same cell can exhibit significant differences in R_{abs} requires that each of these points be calibrated independently. However, because the level of trial-to-trial variability of the $R_{abs(0)}$ documented here was insignificant, it is only necessary to determine this parameter once per experiment. There are several techniques that can be used to determine spatially resolved measurements of $R_{abs(0)}$. For instance, microelectrode measurements (voltage or current clamp) can be made at the conclusion of the experiment to manipulate or verify membrane potential at each point of interest. More practically, pore-forming K^+-selective ionophores such as valinomycin can be used to collapse membrane potential throughout the whole cell, after which $R_{abs(0)}$ can be determined directly. This approach has been successfully used to calibrate optical measurements of membrane potential (Bedlack et al., 1994) and is analogous to the chemical calibrations commonly undertaken with the Ca^{2+} indicator Fura-2 (Grynkiewicz et al., 1985).

Comparison with previous emission ratio methods

Although the possibility for emission ratiometric methods was apparent from early studies characterizing this class of VSDs (see Figs. 2 and 3, Fluhler et al., 1985), only two subsequent studies have attempted to employ the emission shift as the basis for such measurements. Initially, Beach et al. (1996) examined membrane potential changes in perfused arterioles during vasomotor responses. These authors correlated ratiometric optical signals from di-8-ANEPPS measured at a single site ($\sim$100 μm diameter) with microelectrode recordings and demonstrated strong similarity between the two. However, the maximum rate at which these signals could be acquired (after necessary filtering) was only 5 Hz, and these authors reported an uncertainty of 15% in the accuracy of these recordings. Furthermore, representative records documented in this paper exhibited only modest signal-to-noise performance (i.e., S/N $\sim$2). However, an important advantage of this approach apparent from their study was that these measurements were tolerant to movement of the preparation, as simultaneous ratio formation served to cancel out any movement artifacts. Recently, Rohr and Kucera (1998) have used a similar approach to overcome movement artifacts generated by the contractile behavior of cardiac myocyte cultures.

Yuste et al. (1997) employed the emission spectral shift of di-4-ANEPPS to undertake quantitative imaging of gross electrical activity in cortical brain slices from rat. This study documented some of the technical problems inherent in applying this voltage-sensitive dye to complex multicellular preparations and how emission ratio measurements were useful in overcoming some of these limitations. For instance, these authors noted two different signal components (i.e., fast and slow) arising from their brain slices after electrical stimulation. Only one of these components was voltage dependent. Furthermore, preliminary studies (Denk et al., 1994) with two-photon imaging techniques revealed a heterogeneous staining pattern and a considerable degree of internalization after staining with this dye. The emission ratio technique used by these authors helped alleviate both of these problems. However, it was still difficult to accurately determine what proportion of their signals was due to plasma membrane signals from principal cells, and thus the meaning of these signals is difficult to interpret. Moreover, the frame rate of the cooled CCD imaging camera used in this study limited the useful temporal bandwidth that could be achieved.

Neither of these two studies (i.e., Beach et al., 1996, and Yuste et al., 1997) used ratiometric measurements to derive

an absolute calibration factor from which a signal in millivolts was generated. Instead, Beach et al. (1996) used this method to equate $\Delta F/F$ with a change in membrane potential without reference to resting membrane potential. Likewise, Yuste et al. (1997) presented their imaging data as $\Delta F/F$ (although it is functionally equivalent to $\Delta R/R$, as described in this paper).

Another advantage of the approach proposed here is the detector options arising from the combination of random-access scanning and dual-emission detection. Because spatial resolution under these conditions is derived from a small and accurately positioned scanning spot, instead of an imaging device, the detectors employed can be quite simple (i.e., single photodiode) and inexpensive. Furthermore, there is no requirement to mechanically align two imaging detectors, which can be quite difficult, especially with high-resolution devices such as CCD cameras.

In summary, when compared to previous studies using emission ratio techniques, our approach exhibits faster acquisition rates, greater relative spatial resolution, and better voltage discrimination. Furthermore, this approach yielded a higher signal signal-to-noise ratio than earlier studies. Finally, in contrast to these other studies, we were able to calibrate this method under conditions that optimize experimental control and measurement accuracy.

Comparison with existing excitation ratio methods

Initially, the possibility of ratiometric membrane potential measurements based on an excitation shift was shown by Montana et al. (1989), who used di-4-ANEPPS in lipid vesicles and HeLa cells to show the feasibility of this concept. Later, Loew and colleagues conducted a number of studies that utilized the excitation spectral shift of di-8-ANEPPS (Bedlack et al., 1992, 1994; Gross et al., 1994). Most recently, these authors have undertaken experiments, in isolated cells, equivalent to those conducted here (Zhang et al., 1998). This study employed an imaging camera (i.e., cooled CCD) and patch-clamp techniques to definitely calibrate the optical signals. Like the current study, they found it necessary to normalize the ratio value to that measured at zero membrane potential. These authors speculated that the variability in R_{abs}, measured using excitation ratio formation, could be due to regional differences in dipole potential (Zhang et al., 1998). A previous study from this same group (Gross et al., 1994) had shown that localized signals from di-8-ANEPPS are quite sensitive to this parameter.

The determinations made by Zhang et al. (1998) yielded a calibration factor larger than that measured here (0.15 versus 0.015 per 100 mV), although different normalization procedures make an absolute comparison difficult. The relative change in the ratio was much closer (i.e., 15% versus 8% per 100 mV). This discrepancy likely arises from differences in the relative size of the excitation shift, which is larger than the emission shift. Another possibility is that

because these authors used broadband detection (>570 nm), it is likely that the emission shift also contributed somewhat to the relative change in fluorescence they measured. Potentially, some fraction of these differences also arose from variations in voltage sensitivity exhibited by each cell type (Ross and Reichardt, 1979). Finally, the mechanism used by Zhang et al. (1998) to normalize their ratiometric measurements (i.e., division of a line by a constant value) may have also changed the slope of the ratio versus membrane potential relationship and hence artificially changed the underlying voltage sensitivity. Despite these facts, this study elegantly demonstrated the utility of ratiometric methods in making quantitative measurements of membrane potential and the importance of undertaking an electrical calibration. However, because of the nature of the detector used and the necessity to switch excitation filters, the maximum temporal bandwidth possible with this approach is insufficient to follow fast membrane potential events (i.e., action potentials), and therefore the biological usefulness of this method is limited to static determinations. Furthermore, because such measurements are not simultaneous, their method is unable to benefit from the noise cancellation features of the approach used in this study.

Limitations and trade-offs

This report documents an important advance in the application of laser scanning microscopy to the study of fast membrane potential events with VSDs. However, there are a number of considerations that limit the usefulness of this approach and the extent to which it can be generalized to other experimental situations.

In particular, a number of trade-offs were made in the design and implementation of the instrumentation used here. Specifically, the need to obtain images and physiological signals simultaneously has been circumvented. Instead, we have chosen to utilize a stationary differential interference contrast (DIC) image to select points for further study under conditions that maximize temporal resolution and provide a higher signal-to-noise ratio from indicators such as VSDs. This trade-off has also allowed us to record with high spatial resolution while maintaining a large temporal bandwidth and optimizing signal-to-noise considerations for two independent signals from the same fluorophore.

Furthermore, various properties of the VSDs, and di-8-ANEPPS in particular, should be highlighted as potential limitations. First, it has been noted in several studies that significant differences exist in the response of these dyes based on species, cellular, and subcellular characteristics (Bedlack et al., 1994; Ross and Reichardt, 1979; Zhang et al., 1998). In the current study, this observation strongly influences the selection of the secondary emission dichroic, which is dependent on the magnitude of voltage-dependent shifts that arise from membrane potential. For instance, Beach et al. (1996) found that the voltage-insensitive point in the emission difference spectrum of di-8-ANEPPS was

> 590 nm, whereas Yuste et al. (1997) document a value of 590 nm for the parameter in the closely related probe di-4-ANEPPS. We found this point to be between 570 and 580 nm for di-8-ANEPPS. These differences are, of course, in addition to variations arising from underlying differences in the resting membrane potential of the cell.

A second limitation arising from the use of bath-applied VSDs is the magnitude of nonspecific fluorescence arising from surrounding cellular structures or dye bound in a nonspecific orientation. In our study, the magnitude of this nonspecific fluorescence was minimized by the use of a relatively sparse preparation of cultured neurons and by the high-resolution, point-scanning capability inherent in our instrument. Moreover, because these probes undergo a spectral shift upon membrane binding, the effect of nonspecific fluorescence can be minimized by the inclusion of a narrow-band emission filter (rather than a long-pass filter) in the long-wavelength detector pathway, as we have done. Restriction of the optical bandwidth of this signal reduces the contribution of dye not bound to the membranes of healthy cells and thus increases the specificity of the measured responses. However, any remaining nonspecific fluorescence will almost exclusively contribute to the long-wavelength component of the ratio and thus would compromise calibration accuracy. Unfortunately, the magnitude of nonspecific fluorescence inherent in complex, multicellular tissues would make the straightforward application of this technique to such preparations difficult (but see the next section). However, it is conceivable that this problem could also be alleviated through the use of the confocal or two-photon microscopy, which excludes the contribution of out-of-focus fluorescence.

A related issue is the resolution and the signal-to-noise ratio achieved with the parameter R_{norm}. The voltage sensitivity of R_{norm} is relatively less than some published values (Rohr and Salzberg, 1994a,b) measured using only single-wavelength detection (i.e., $\Delta F/F$). This observation probably arises because the relative signal size of the ratio (i.e., $\Delta R_{abs}/R_{abs}$) is smaller than the maximum $\Delta F/F$ possible. This likely occurs because a simple $\Delta F/F$ measurement, under the appropriate conditions, can take advantage of both amplitude changes and spectral shifts (in both excitation and emission) to generate a larger relative change in fluorescence (see Fig. 1 B). Although it should be noted that these limitations can be overcome, in large part, by the increase in dynamic range of the ratio and noise cancellation feature that arises through the ratio formation process, it is nonetheless interesting that the optimal excitation wavelength from a signal-to-noise standpoint is likely different for ratiometric and nonratiometric measurements.

Finally, spectral changes other than simple voltage shifts are known to occur in both excitation and emission spectra, and this can potentially detract from the accuracy and precision of measurements made in this manner. For instance, the magnitude of the fluorescence signals arising from the spectral band less than 570 nm is thought to decrease somewhat after depolarization, and this likely complicates the ratio formation process (Fromherz and Lambacher, 1991), although the degree to which it does this is unclear.

Future developments

It is conceivable that similar ratiometric methods based on voltage-dependent emission shifts could be applied to other preparations and/or VSDs. Most VSDs in the styryl dye family exhibit some degree of emission shift (Fromherz and Lambacher, 1991; Fromherz and Muller, 1993), although not always in the same direction. One particularly interesting candidate would be the intracellular dye di-2-ANEPEQ, which has been successfully used in neurons from snail ganglia (Antic and Zecevic, 1995; Zecevic, 1996). This dye possesses a fluorophore that is structurally similar to di-8-ANEPPS. The capability of making ratiometric measurements with such an intracellular VSDs would considerably reduce the problem of nonspecific fluorescence discussed in the previous section. Our preliminary experiments with di-2-ANEPEQ in cultured hippocampal neurons (Bullen and Saggau, unpublished results) indicate that ratiometric measurements can be made with this indicator in the manner we have described in this paper. However, the extension of this approach to more complex preparations awaits further experimentation.

This instrument would also be useful for recording fast ion transients with two indicators that have distinct spectra and signals that change in opposite directions. For example, ratiometric calcium measurements could be made with a green-emitting indicator (e.g., Calcium Green, Fluo-3 or Oregon Green) and a red-emitting probe (e.g., Fura Red), as has been proposed previously by Lipp and Niggli (1993).

SUMMARY AND CONCLUSIONS

In summary, we have successfully demonstrated the ability to record quantitative optical signals from fine neuronal structures at high temporal resolution, using a high-speed, random-access, laser-scanning fluorescence microscope. This achievement is significant because it overcomes many of the limitations inherent in previous attempts to make multisite ratiometric recordings with VSDs. Furthermore, these improvements also overcome many of the inherent limitations of classical electrophysiological approaches and will thus facilitate future investigations into a wide range of neurobiological issues.

REFERENCES

Antic, S., and D. Zecevic. 1995. Optical signals from neurons with internally applied voltage-sensitive dyes. *J. Neurosci.* 15:1392–1405.

Beach, J. M., E. D. McGahren, J. Xia, and B. R. Duling. 1996. Ratiometric measurement of endothelial depolarization in arterioles with a potential-sensitive dye. *Am. J. Physiol.* 39:H2216–H2227.

Bedlack, R. S., M.-D. Wei, S. H. Fox, E. Gross, and L. M. Loew. 1994. Distinct electric potentials in soma and neurite membranes. *Neuron.* 13:1187–1193.

Bedlack, R. S., M.-D. Wei, and L. M. Loew. 1992. Localized membrane depolarizations and localized calcium influx during electric field-guided neurite growth. *Neuron.* 9:393–403.

Brewer, G. J., J. R. Torricelli, E. K. Evege, and P. J. Price. 1993. Optimized survival of hippocampal neurons in B27-supplemented NeuroBasal, a new-serum-free combination. *J. Neurosci. Res.* 35:567–576.

Bullen, A., S. S. Patel, and P. Saggau. 1997. High-speed, random-access fluorescence microscopy. I. High resolution optical recording with voltage-sensitive dyes and ion indicators. *Biophys. J.* 73:477–491.

Bullen, A., and P. Saggau. 1997a. Fast ratiometric measurements of membrane potential using a voltage-sensitive dye and high-speed, random-access, laser-scanning microscopy. *Biophys. J.* 72:A24.

Bullen, A., and P. Saggau. 1997b. Fast membrane potential dynamics determined by ratiometric fluorescence measurements using a voltage-sensitive dye and high-speed, random-access, laser-scanning microscopy. *Soc. Neurosci. Abstr.* 23:865.6.

Cohen, L. B., and B. M. Salzberg. 1978. Optical methods for monitoring neuron activity. *Annu. Rev. Neurosci.* 1:171–182.

Denk, W., K. R. Delaney, A. Gelperin, D. Kleinfeld, B. W. Strowbridge, D. W. Tank, and R. Yuste. 1994. Anatomical and functional imaging of neurons using two-photon laser scanning microscopy. *J. Neurosci. Methods.* 54:151–162.

Dunn, K. W., S. Mayor, J. N. Myers, and F. R. Maxfield. 1994. Applications of ratio fluorescence microscopy in the study of cell physiology. *FASEB J.* 8:573–582.

Ebner, T. J., and G. Chen. 1995. Use of voltage-sensitive dyes and optical recordings in the central nervous system. *Prog. Neurobiol.* 46:463–506.

Ehrenberg, B., D. L. Farkas, E. N. Fluhler, Z. Lojewska, and L. M. Loew. 1987. Membrane potential induced by external electric field pulses can be followed with a potentiometric dye. *Biophys. J.* 51:833–837.

Fluhler, E. N., V. G. Burnham, and L. M. Loew. 1985. Spectra, membrane binding and potentiometric responses of new charge shift probes. *Biochemistry.* 24:5749–5755.

Fromherz, P., and A. Lambacher. 1991. Spectra of voltage-sensitive fluorescence of styryl dye in neuron membrane. *Biochim. Biophys. Acta.* 1068:149–156.

Fromherz, P., and C. O. Muller. 1993. Voltage-sensitive fluorescence of amphiphilic hemicyanine dyes in neuron membrane. *Biochim. Biophys. Acta.* 1150:111–122.

Fromherz, P., and C. O. Muller. 1994. Cable properties of a straight neurite of a leech neuron probed by a voltage-sensitive dye. *Proc. Natl. Acad. Sci. USA.* 91:4604–4608.

Gonzalez, J. E., and R. Y. Tsien. 1995. Voltage sensing by fluorescence resonance energy transfer in single cells. *Biophys. J.* 69:1272–1280.

Gonzalez, J. E., and R. Y. Tsien. 1997. Improved indicators of cell membrane potential that use fluorescence resonance energy transfer. *Chem. Biol.* 4:269–277.

Goslin, K., and G. Banker. 1991. Rat hippocampal neurons in low-density culture. *In* Culturing Nerve Cells. G. Banker, editor. MIT Press, Cambridge, MA.

Gross, E., R. S. Bedlack, and L. M. Loew. 1994. Dual-wavelength ratiometric fluorescence measurement of the membrane dipole potential. *Biophys. J.* 67:208–216.

Grynkiewicz, G., M. Poenie, and R. Y. Tsien. 1985. A new generation of Ca^{++} indicators with greatly improved fluorescence properties. *J. Biol. Chem.* 260:3440–3450.

Haugland, R. P. 1996. Handbook of Fluorescent Probes and Research Chemicals. Molecular Probes, Eugene, OR.

Lipp, P., and E. Niggli. 1993. Ratiometric Ca^{2+} measurements with visible wavelength indicators in isolated cardiac myocytes. *Cell Calcium.* 14:359–372.

Loew, L. M. 1993. Potentiometric membrane dyes. *In* Fluorescent and Luminescent Probes for Biological Activity. W. T. Matson, editor. Academic Press, London. 150–160.

Loew, L. M., L. B. Cohen, J. Dix, E. N. Fluhler, V. Montana, G. Salama, and W. Jian-Young. 1992. A naphthyl analog of the aminostyryl pyridinium class of potentiometric membrane dyes shows consistent sensitivity in a variety of tissue, cell and model membrane preparations. *J. Membr. Biol.* 130:1–10.

Loew, L. M., L. B. Cohen, B. M. Salzberg, A. L. Obaid, and F. Bezanilla. 1985. Charge-shift probes of membrane potential: characterization of aminostyrylpyridinium dyes on the squid giant axon. *Biophys. J.* 47:71–77.

Loew, L. M., S. Scully, L. Simpson, and A. S. Waggoner. 1979. Evidence for a charge-shift electrochromic mechanism in a probe of membrane potential. *Nature.* 281:497–499.

Montana, V., D. L. Farkas, and L. M. Loew. 1989. Dual-wavelength ratiometric fluorescence measurements of membrane potential. *Biochemistry.* 28:4536–4539.

Obaid, A. L., and B. M. Salzberg. 1997. Optical studies of an enteric plexus: recording the spatio-temporal patterns of activity of an intact network during electrical stimulation and pharmacological interventions. *Soc. Neurosci. Abstr.* 816.1. 23(2):2097.

Rohr, S., and J. P. Kucera. 1998. Optical recording system based on a fiber optic image conduit: assessment of microscopic activation patterns in cardiac tissue. *Biophys. J.* 75:1062–1075.

Rohr, S., and B. M. Salzberg. 1994a. Multiple site optical recording of transmembrane voltage (MSORTV) in patterned growth heart cell cultures: assessing electrical behavior, with microsecond resolution, on a cellular and subcellular scale. *Biophys. J.* 67:1301–1315.

Rohr, S., and B. M. Salzberg. 1994b. Characterization of impulse propagation at the microscopic level across geometrically defined expansions of excitable tissues: multiple site optical recording of transmembrane voltage (MSORTV) in pattern growth heart cell cultures. *J. Gen. Physiol.* 104:287–309.

Ross, W. N., and L. F. Reichardt. 1979. Species-specific effects on the optical signals of voltage-sensitive dyes. *J. Membr. Biol.* 48:343–356.

Salzberg, B. M., A. L. Obaid, and F. Bezanilla. 1993. Microsecond response of a voltage-sensitive merocyanine dye: fast voltage-clamp measurements on squid giant axon. *Jpn. J. Physiol.* 43:37–41.

Scheenen, W. J. J. M., L. R. Makings, L. R. Gross, T. Pozzan, and R. Y. Tsien. 1996. Photodegradation of indo-1 and its effect on apparent Ca^{2+} concentrations. *Chem. Biol.* 3:765–774.

Tsien, R. Y., and M. Ponnie. 1986. Fluorescence ratio imaging: a new window into intracellular ionic signaling. *Trends Biochem. Sci.* 11:450–455.

Yuste, R., D. W. Tank, and D. Kleinfeld. 1997. Functional study of the rat cortical microcircuitry with voltage-sensitive dye imaging of neocortical slices. *Cerebral Cortex.* 7(6):546–558.

Zecevic, D. 1996. Multiple spike-initiation zones in single neurons revealed by voltage-sensitive dyes. *Nature.* 381:322–325.

Zhang, J., R. M. Davidson, M.-D. Wei, and L. M. Loew. 1998. Membrane electric properties by combined patch clamp and fluorescence ratio imaging in single neurons. *Biophys. J.* 74:48–53.